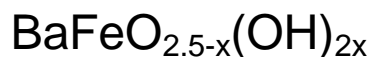# *Electronic Supplementary Information for*

# Synthesis, structural characterisation and proton conduction of two new hydrated phases of barium ferrite BaFeO$_{2.5-x}$(OH)$_{2x}$

Patrick L. Knöchel[a], Philip J. Keenan[b], Christoph Loho[a,c], Christian Reitz[c], Ralf Witte[c], Kevin S. Knight[d], Adrian J. Wright[b], Horst Hahn[a,c], Peter R. Slater[b], Oliver Clemens[a,c,*]

a) Technical University of Darmstadt, Joint Research Laboratory Nanomaterials, Jovanka-Bontschits-Straße 2, 64287 Darmstadt, Germany.

b) University of Birmingham, School of Chemistry, Edgbaston, Birmingham B15 2TT, United Kingdom.

c) Karlsruhe Institute of Technology, Institute of Nanotechnology, Hermann-von-Helmholtz-Platz 1, 76344 Eggenstein-Leopoldshafen, Germany.

d) ISIS Facility, Rutherford Appleton Laboratory, Harwell Oxford, Didcot, OX11 0QX, United Kingdom.

* Corresponding Author

Fax: +49 6151 16 6335

E-Mail: oliver.clemens@kit.edu

# Results of Pawley fits for the symmetry analysis of LW-BaFeO$_{2.5}$

**Table S 1. Orthorhombic C-centered space groups which can be distinguished according to systematic absences of reflections [1]. All space groups relate to a cell parameter setting of 6a$_{cub}$ x 2$\sqrt{2}$a$_{cub}$ x $\sqrt{2}$a$_{cub}$. \* := space group numbers / symbols given in parentheses are non-centrosymmetric direct subgroups of the highest symmetric centrosymmetric representative of the respective row.**

| space group numbers / symbols with identical hkls* | most significant misfit due to which those space groups can (might) be ruled out from Pawley fits | combined R$_{wp}$ of Pawley fit [%] |
|---|---|---|
| 68 / *Ccca* | Reflection group with d-spacing of ~ 4.1 Å can't be fitted appropriately for the neutron data as well as for the XRD data (splitted (0 0 1)$_{cub}$ main reflection) | 3.43 |
| 63 (40, 36) / *Ccmm* (*Aam*2, *Ccm*2$_1$) | | 3.40 |
| 66 (37) / *Cccm* (*Ccc*2) | | 3.46 |
| 64 (41) / *Cmce* (*Aea*2) | XRD superstructure reflection (1 1 0) at d ~ 10.7 Å prohibited by this symmetry, position misfit of reflection in detector bank 2 at d ~ 2.0 Å | 2.90 |
| 67 (39) / *Cmma* (*Abm*2) | | 2.88 |
| 63 (40, 36) / *Cmcm* (*Ama*2, *Cmc*2$_1$) | none | 2.84 |
| 65 (38, 35, 21) / *Cmmm* (*Amm*2, *Cmm*2, *C*222) | | 2.80 |

(a) LW-BaFeO$_{2.5}$, XRD pattern recorded at ambient temperature; 2theta vs. Intensity (broad reflection at ~24° 2theta belongs to BaCO$_3$)
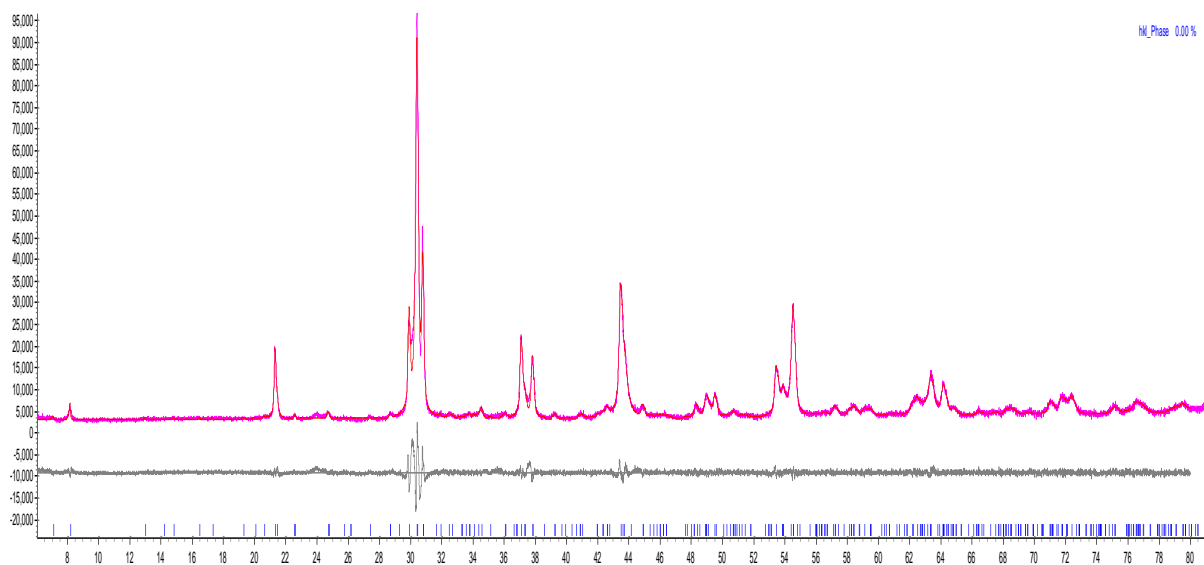


(b) LW-BaFeO$_{2.5}$, TOF neutron diffraction data recorded at HRPD at T = 423 K, bank 1, TOF [μsec] vs. Intensity [a.u.]
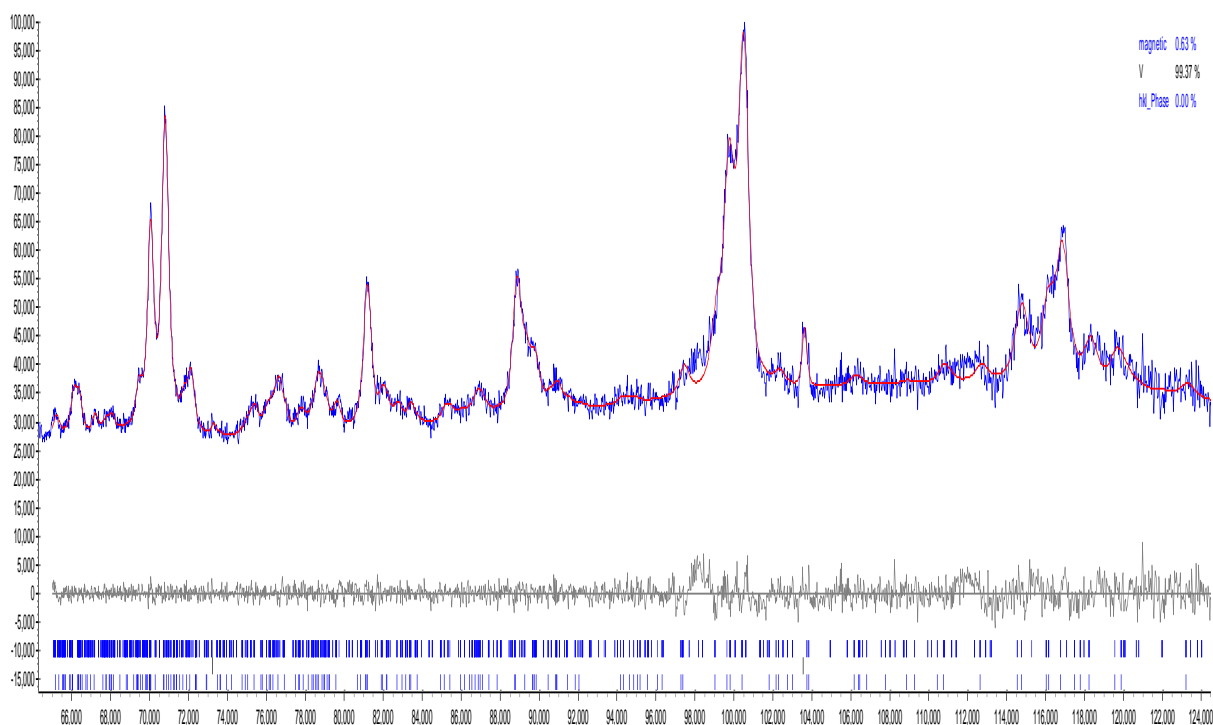
(c) LW-BaFeO$_{2.5}$, TOF neutron diffraction data recorded at HRPD at T = 423 K, bank 2, [µsec] vs. Intensity [a.u.]
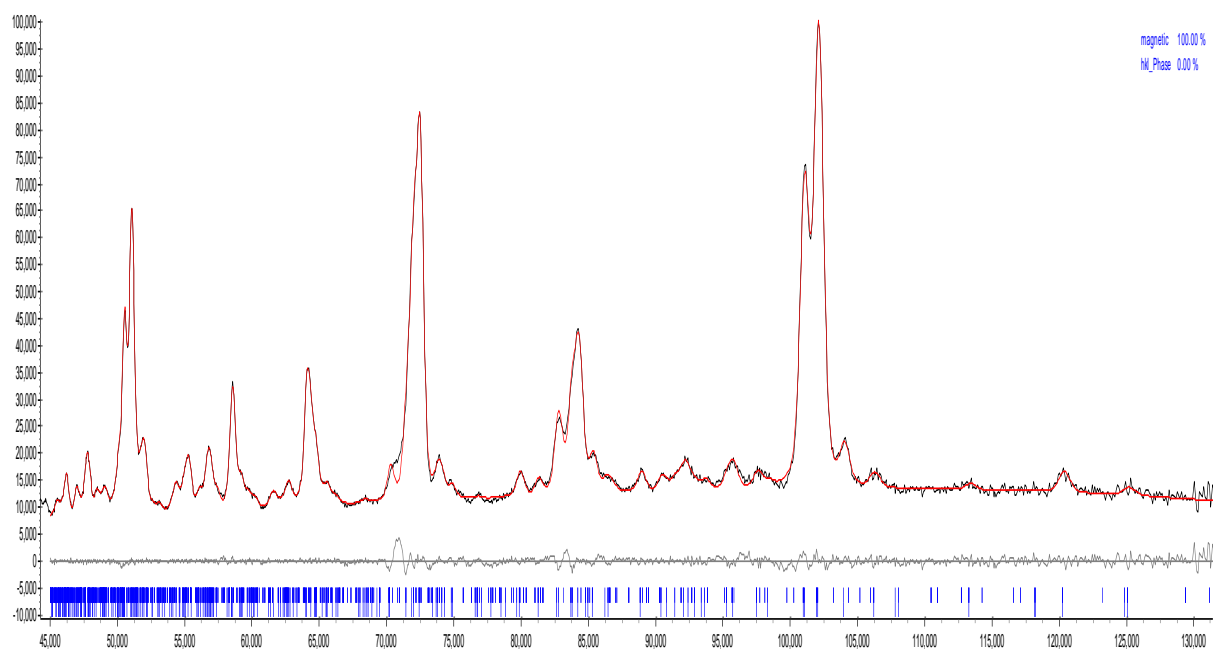


(d) LW-BaFeO$_{2.5}$, TOF neutron diffraction data recorded at HRPD at T = 423 K, bank 2, [µsec] vs. Intensity [a.u.]



**Figure S 1. Results of Pawley Fits performed with space group Cmcm on the patterns of LW-BaFeO$_{2.5}$ recorded at ambient temperature ((a), XRD), and 423 K ((b), (c), (d) NPD).**

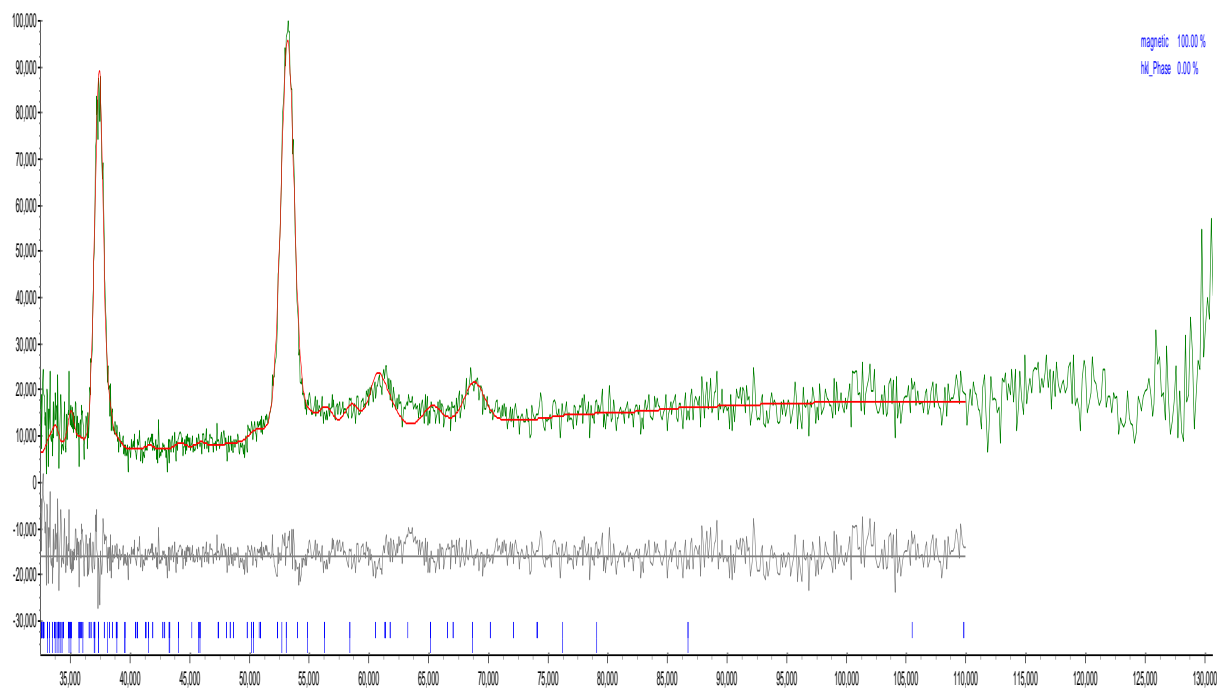# Symmetry tree for relating the structure of LW-BaFeO$_{2.5}$ to the cubic perovskite type structure

Cubic
*Pm-3m* (221)
$a_1 = 4.10$ Å

$t4$ $\quad a_2 = a_1$
$\quad b_2 = b_1$
$\quad c_2 = c_1$

Tetragonal
*P4/mmm* (123)
$a_2 = 4.10$ Å
$c_2 = 4.10$ Å

$i3$ $\quad a_3 = a_2$
$\quad b_3 = b_2$
$\quad c_3 = 3c_2$

Tetragonal
*P4/mmm* (123)
$a_3 = 4.10$ Å
$c_3 = 12.30$ Å

$t2$ $\quad a_4 = a_3 - b_3$
$\quad b_4 = a_3 + b_3$
$\quad c_4 = c_3$

Orthorhombic
*Cmmm* (65)
$a_4 = 5.80$ Å
$b_4 = 5.80$ Å
$c_4 = 12.30$ Å

$a_5 = b_4$ $\quad$ $a_5 = a_4$
$b_5 = c_4$ $k2$ $\quad$ $k2$ $\quad$ $b_5 = b_4$
$c_5 = a_4$ $\quad$ $c_5 = c_4$

Orthorhombic
*Pmma* (51)
$a_5 = 5.80$ Å
$b_5 = 12.30$ Å
$c_5 = 5.80$ Å

Orthorhombic
*Pmmm* (47)
$a_5 = 5.80$ Å
$b_5 = 5.80$ Å
$c_5 = 12.30$ Å

$a_6 = 2b_5$ $\quad$ $a_6 = 2c_5$
$b_6 = 2c_5$ $k2$ $\quad$ $k2$ $\quad$ $b_6 = 2a_5$
$c_6 = a_5$ $\quad$ $c_6 = b_5$

Orthorhombic
*Cmcm* (63)
$a_6 = 24.60$ Å
$b_6 = 11.60$ Å
$c_6 = 5.80$ Å

Orthorhombic
*Cmmm* (65)
$a_6 = 24.60$ Å
$b_6 = 11.60$ Å
$c_6 = 5.80$ Å

(a)

(b)

## *Cmcm* - Structure 1
Ba → 2 x 4*c*, 2 x 8*g*
Fe → 3 x 8*g*
O → 2 x 4*c*, 8*d*, 3 x 8*e*, 8*f*, 2 x 8*g*, 16*h*

## *Cmcm* - Structure 2
Ba → 3 x 8*g*
Fe → 2 x 4*c*, 2 x 8*g*
O → 4*a*, 4*b*, 2 x 8*e*, 8*f*, 3 x 8*g*, 16*h*

## *Cmmm* - Structure 1
Ba → 2*c*, 2*d*, 4*i*, 2 x 4*h*, 8*p*
Fe → 4*f*, 3 x 4*g*, 8*q*
O → 2*a*, 2*b*, 2 x 4*g*, 4*j*, 8*q*, 3 x 16*r*

## *Cmmm* - Structure 2
Ba → 4*f*, 3 x 4*g*, 8*q*
Fe → 2*c*, 2*d*, 4*i*, 2 x 4*h*, 8*p*
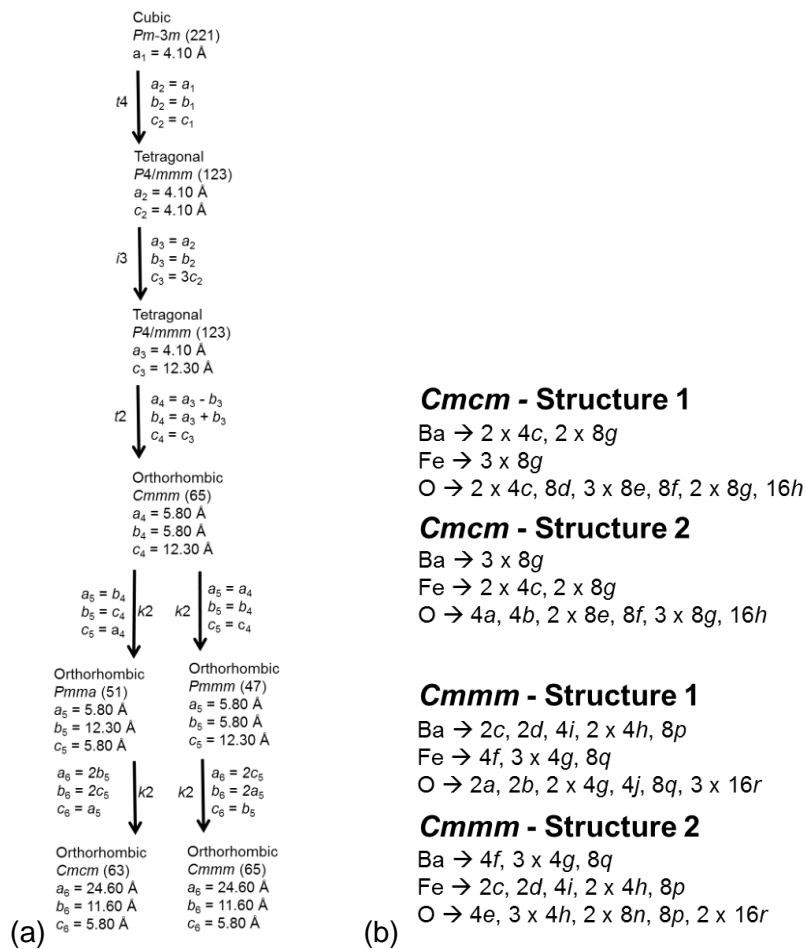O → 4*e*, 3 x 4*h*, 2 x 8*n*, 8*p*, 2 x 16*r*

**Figure S 2. (a) Symmetry tree for the relationship of the superstructure found for LW-BaFeO$_{2.5}$ to the cubic perovskite structure. (b) Splitting of atomic sites into crystallographically independent Wyckoff sites for the different structures within orthorhombic space groups *Cmcm* and *Cmmm*.**

# Discussion of the structural model of LW-BaFeO$_{2.5}$ in comparison to other vacancy ordered modifications of barium ferrite

The following reasons detail why structure 1 with *Cmcm* symmetry must indeed be considered to be the best approximation to the real structure and symmetry of LW-BaFeO$_{2.5}$. This discussion will also help the reader to understand why the structural models with symmetry of *Cmmm* must be considered to be implausible from structure chemical considerations. Clemens [2] has already provided a detailed discussion of such factors for Fe$^{3+}$ containing compounds in a recent article, and the observations made are summarized in the following. With respect to the compositions of the hydrated phases of BaFeO$_{2.5}$, a strong deficiency of anions is still indicated ($\sim \frac{1}{9}$ of the anion sites would be expected to be empty for LW-BaFeO$_{2.5}$). Such anion deficiency often results in the ordering of anion vacancies, i. e. very distinct crystallographic anion sites remain completely vacant. It is acknowledged at this point that compounds with random disorder of the anion lattice (but locally lowered coordination number), e. g. BaCoO$_{\sim2.2}$ [3], are also known, but such disorder then most often results in the observation of the very simple diffraction pattern of the cubic perovskite structure, which is clearly not the case for the hydrated phases of BaFeO$_{2.5}$. Let us therefore assume that the structural distortion found for LW- BaFeO$_{2.5}$ will indeed be related to a complete ordering of anion vacancies. Regarding the splitting of the anion sites for both symmetries, *Cmcm* and *Cmmm*, such a completely vacancy ordered structure with composition BaFeO$_{2.333}$(OH)$_{0.333}$ could be easily obtained by leaving e. g. one of the sites with 8-fold or two of the sites with 4-fold multiplicity empty. Apart from the splitting of the anion sites, one also needs to consider possible structural relaxation mechanisms around the vacancy formed, resulting in a change in the coordination of the B- (as well as A-) site cations and stabilization of the structural arrangement. In this respect it is of high importance to consider coordination environments which are usually found for Fe$^{3+}$ containing compounds. The predominant vacancy formation mechanism is related to the brownmillerite type, with channels of anion vacancies along the [1 1 0]$_{cub}$ direction (for the group-subgroup-relationship between the cubic perovskite type structure and the brownmillerite type structure, see e. g. [4]). Such ordering facilitates the formation of tetrahedral coordination environments for some of the B-cations, which can order either 1) layer like (e. g. found for the brownmillerite type compounds CaFeO$_{2.5}$ and SrFeO$_{2.5}$, see Figure S 3a), 2) along different [1 1 0]$_{cub}$ type directions (e. g. as found for BaFeO$_{2.5}$, see Figure S 3b), or 3) along the same [1 1 0]$_{cub}$ type direction in different layers (as e. g. found for BaFeO$_{2.333}$F$_{0.333}$, see Figure S 3c). In the brownmillerite type structures found for the Ca and Sr compounds, the vacancies are further stabilized by a strong tilting of the octahedra within the octahedrally coordinated layers, resulting in a lowering of the effective coordination number (ECoN [5]) of

the A-site cations. However, for the larger Ba-cations, such lowering of the coordination number must be considered to be energetically less favourable. Therefore, for the barium ferrites $BaFeO_{2.5}$ and $BaFeO_{2.333}F_{0.333}$, the A-site coordination is further stabilized by a strong shift of the anion which connects the tetrahedron to the octahedron of the adjacent layer (see Figure S 3d), resulting in square-pyramidal coordination for the former octahedrally coordinated Fe-ion, and accompanied by a further shift of the barium ions towards this shifted anion. Remarkably, the shifted anion would have formerly not contributed to the coordination environment of the respective barium ion, and hence helps to keep the coordination number of the A-site cation high.
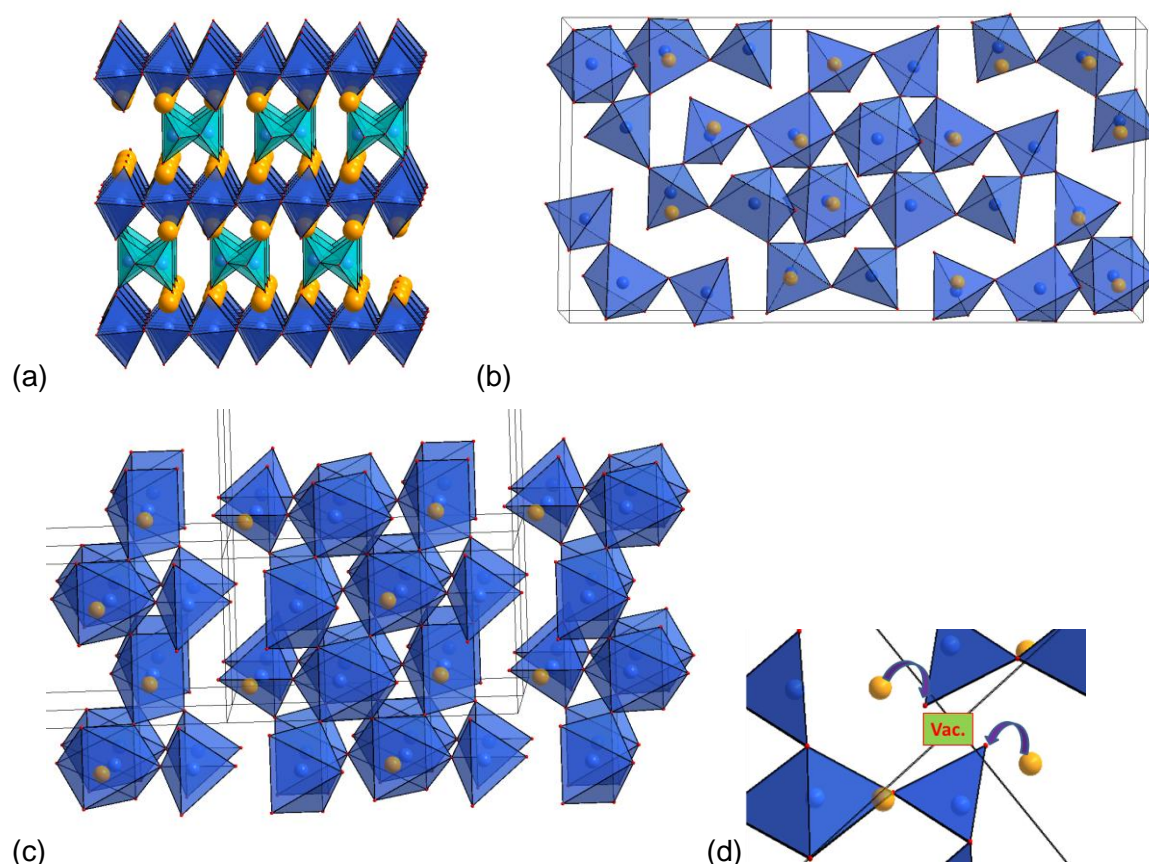


**Figure S 3. Structural relaxation mechanisms found for $Fe^{3+}$ containing compounds: Brownmillerite type $SrFeO_{2.5}$ (a), $BaFeO_{2.5}$ (b), and $BaFeO_{2.333}F_{0.333}$ (c), (d).**

Keeping this in mind, one can now discuss in which respect structure-chemically sensible coordination geometries of the Fe ions can be obtained if distinct anion sites within the *Cmcm* and *Cmmm* type are vacant, which will help to understand from a more qualitative point of view why the *Cmmm* type structure cannot be used to obtain a proper fit of the pattern. The structurally favourable tetrahedral coordination for part of the $Fe^{3+}$ ions can only be obtained if two anions which form the edge of an octahedron are being removed. For an overall composition of $BaFeO_{2.333}(OH)_{0.333}$, this would imply that an edge of an octahedron is

formed by two anions of the same crystallographic site for a site with 8-fold, or by two different sites with 4-fold multiplicity (removing all the anions of a site with 16-fold multiplicity automatically results in an implausibly low overall anion content). For the *Cmmm* symmetry, this octahedron-edge type coordination situation is given neither for structure 1 nor for structure 2, and removal of distinct oxide sites can only result in the formation of linear 2-fold (never found so far), square-planar 4-fold (only found for electronically stabilized Ruddlesden-Popper type Sr-Ru-$Fe^{3+}$ compounds [6]) and unshielded $CaMnO_{2.5}$ type 5-fold coordination of the $Fe^{3+}$ ions (only found for compounds with $Y^{3+}$ on the A-site lattice due to strong reduction of the Y-coordination number; for a more detailed discussion see [2]). Those structural considerations give reasonable support as to why the *Cmmm* space group can be discarded as being unable to correctly describe the symmetry for the hydrated phases of $BaFeO_{2.5}$.

Within the *Cmcm* symmetry, both structures 1 and 2 (see Figure S 2b), allow for the formation of tetrahedrally coordinated Fe ions. Structure 1 allows for brownmillerite type layer-wise ordering of the vacancies, while vacancies are distributed between two thirds of the layers in structure 2. Apart from the lower quality of the fit, the structure model 2 also results in less plausible bond distances for the Fe cations with a less plausible shifting scheme of the Fe cations within their coordination polyhedra.

# Anisotropic thermal parameters found for LW-BaFeO$_{2.5}$

**Table S 2. Anisotropic thermal parameters refined for LW-BaFeO$_{2.5}$.**

| atom | U$_{11}$ | U$_{22}$ | U$_{33}$ | U$_{12}$ | U$_{13}$ | U$_{23}$ |
|------|----------|----------|----------|----------|----------|----------|
| Ba1 | 0.098(13) | 0.015(6) | 0.000(5) | -0.008(9) | -0.003(16) | 0.053(7) |
| Ba2 | 0.000(7) | 0.000(7) | 0.094(10) | 0.002(8) | -0.00(4) | -0.02(3) |
| Ba3 | 0.000(4) | 0.047(3) | 0.000(3) | 0.012(4) | 0.016(12) | -0.008(17) |
| Ba4 | 0.030(4) | 0.054(4) | 0.023(4) | 0.064(3) | -0.01(4) | -0.01(4) |
| Fe1 | 0.000(5) | 0.019(4) | 0.000(4) | 0.031(3) | 0.01(4) | 0.00(5) |
| Fe2 | 0.028(9) | 0.174(11) | 0.082(9) | 0.092(8) | 0.03(3) | 0.01(5) |
| Fe3 | 0.006(4) | 0.001(4) | 0.000(3) | -0.022(4) | -0.011(7) | -0.039(5) |
| O1 | 0.11(3) | 0.32(5) | 0.035(14) | -0.18(4) | 0.01(2) | -0.14(2) |
| O2 | 0.000(14) | 0.012(16) | 0.019(11) | -0.036(15) | 0.01(6) | -0.02(5) |
| O3 | 1.9(2) | 0.41(5) | 0.001(10) | -0.20(11) | 0.01(5) | -0.17(2) |
| O4 | 0.000(7) | 0.033(10) | 0.000(6) | -0.002(7) | 0.017(11) | -0.045(9) |
| O5 | 0.000(8) | 0.000(7) | 0.000(6) | -0.004(5) | -0.021(5) | 0.008(4) |
| O6 | 0.000(7) | 0.002(6) | 0.000(5) | -0.01(3) | -0.01(3) | 0.049(5) |
| O7 | 0.000(8) | 0.104(15) | 0.019(8) | 0.055(13) | 0.038(10) | 0.058(8) |
| O8 | 0.267(17) | 0.082(9) | 1.11(6) | 0.158(10) | 0.58(3) | 0.316(18) |

# References

1.  *Topas V4.2, General profile and structure analysis software for powder diffraction data, User's Manual*, Bruker AXS, Karlsruhe, Germany, 2008.
2.  O. Clemens, *J. Solid State Chem.*, 2015, **225**, 261-270.
3.  O. Mentre, M. Iorgulescu, M. Huve, H. Kabbour, N. Renaut, S. Daviero-Minaud, S. Colis and P. Roussel, *Dalton Trans.*, 2015, DOI: 10.1039/c4dt03874f.
4.  O. Clemens and P. R. Slater, *Rev. Inorg. Chem.*, 2013, **33**, 105-117.
5.  R. Hoppe, *Z. Kristallogr.*, 1979, **150**, 23-52.
6.  F. Denis Romero, D. Gianolio, G. Cibin, P. A. Bingham, J.-C. d'Hollander, S. D. Forder and M. A. Hayward, *Inorg. Chem.*, 2013, **52**, 10920-10928.